

The Noncommutative Standard Model at the ILC

Ana Alboteanu*, Thorsten Ohl, and Reinhold Rückl

Universität Würzburg, Institut für Theoretische Physik und Astrophysik
Am Hubland, 97074 Würzburg, Germany

We study phenomenological consequences of a noncommutative extension of the standard model in the θ -expanded approach at the ILC. We estimate the sensitivity of the ILC for the noncommutative scale Λ_{NC} . Comparing with earlier estimates for the LHC, we demonstrate the complementarity of the experiments at the two colliders.

1 The Model

A noncommutative (NC) structure of space-time

$$[\hat{x}^\mu, \hat{x}^\nu] = i\theta^{\mu\nu} = i\frac{C^{\mu\nu}}{\Lambda_{\text{NC}}^2} \quad (1)$$

introduces a new energy scale Λ_{NC} . The motivations of (1) that are provided by string theory and quantum gravity place this scale in the vicinity of the corresponding Planck scale: $\Lambda_{\text{NC}} \approx M_{\text{Pl}}$. If $M_{\text{Pl}} \approx 10^{19}$ GeV, (1) is unlikely to be ever probed directly by collider experiments. However, in models with additional space dimensions M_{Pl} can be as low as the Terascale and, as a result, Λ_{NC} can be in the reach of future TeV scale colliders, like LHC and ILC. Therefore, quantum field theories on NC space-time (NCQFT), in particular NC extensions of the standard model (SM), are interesting objects for collider phenomenology. Using methods developed for studying NCQFT at the LHC [2], we have estimated the discovery potential of the ILC and the sensitivity to the NC parameters (1).

In this study, we assume a canonical structure of NC space-time, i.e. a constant antisymmetric 4×4 matrix $C^{\mu\nu}$ in (1) that commutes with all the \hat{x}_μ . For convenience, we parametrize $C^{\mu\nu}$ in analogy to the electromagnetic field-strength tensor and denote the time-like components C^{0i} by \vec{E} and the space-like components C^{ij} by \vec{B} . Instead of constructing NCQFT directly in terms of the operators \hat{x} , we encode the NC structure (1) of space-time by means of a deformed product of functions on an ordinary commuting space-time, the so called Moyal-Weyl \star -product:

$$f(x) \star g(x) = f(x) e^{\frac{i}{2} \overleftarrow{\partial}^\mu \theta_{\mu\nu} \overrightarrow{\partial}^\nu} g(x). \quad (2)$$

For the implementation of the gauge structure of the SM, we use the framework introduced in [3], where the Lie algebra valued gauge and matter fields A_ξ and ψ are mapped to universal enveloping algebra valued fields $\hat{A}_\xi[A, \theta]$ and $\hat{\psi}[A, \psi, \theta]$, allowing the $SU(N)$ gauge groups and fractional $U(1)$ -charges of the SM on NC space-time. These so-called Seiberg Witten Maps (SWM) are defined as solutions of the following gauge equivalence equations, that express the requirement that the NC gauge transformations are realized by ordinary gauge transformations:

$$\hat{\delta}_\alpha \hat{A}_\mu(A, \theta) = \delta_\alpha \hat{A}_\mu(A, \theta) \quad (3a)$$

$$\hat{\delta}_\alpha \hat{\psi}(\psi, A, \theta) = \delta_\alpha \hat{\psi}(\psi, A, \theta). \quad (3b)$$

*Speaker [1]

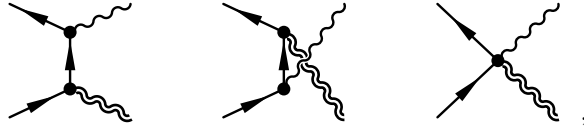
The solutions of (3) can be obtained as an expansion in powers of θ . While we have constructed the most general second order expressions recently [4], we will restrict ourselves here to the first order in θ to be consistent with the existing LHC study [2].

The construction sketched in the previous paragraph introduces momentum dependent corrections to the SM vertices, as well as new vertices that are absent in the SM, e.g. $f\bar{f}VV$ contact interactions among fermions and gauge bosons. In addition, the gauge boson sector of the NCSM shows a new feature, characteristic to the universal algebra valued approach [3]. The action depends on the choice of the representation, resulting in different versions of the model: the minimal NCSM containing no triple couplings among neutral gauge bosons and the nonminimal NCSM, where such triple gauge boson (TGB) couplings, that are forbidden in the SM, appear. The coupling strength of TGB interactions are not uniquely fixed in the nonminimal NCSM, but constrained to a finite domain (see Figure 1, left). An important aspect of our phenomenological analysis is probing different values of these couplings at the ILC and deriving the corresponding sensitivity on the NC scale Λ_{NC} . This will reveal a complementarity with measurements at the LHC.

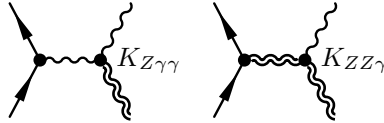
2 Phenomenology

We perform a phenomenological analysis of the unpolarized scattering process $e^+e^- \rightarrow Z\gamma$ in the minimal as well as in the nonminimal NCSM. The final state was selected to contain a Z -boson, since the axial coupling of the Z is crucial for a non-cancellation of the NC effects after summing over polarizations [5, 2].

In the minimal NCSM, the $\mathcal{O}(\theta)$ contribution to the $e^+e^- \rightarrow Z\gamma$ scattering amplitude is given by the diagrams



whereas in the nonminimal NCSM two additional s -channel diagrams



have to be added, introducing a dependence on $K_{Z\gamma\gamma}$ and $K_{ZZ\gamma}$.

2.1 Dependence on the Azimuthal Angle

A NC structure of space-time as introduced in (1), breaks Lorentz invariance, including rotational invariance around the beam axis. This leads to a dependence of the cross section on the azimuthal angle, that is otherwise absent in the SM, as well as in most other models of physics beyond the SM (see Figure 1, right). In principle, we can distinguish \vec{E} -type and \vec{B} -type NC contributions by their different dependence on the polar scattering angle: the differential cross section is antisymmetric in $\cos\vartheta$ for $\vec{E} \neq 0$ and it is symmetric for $\vec{B} \neq 0$. However, the dependence of the cross section on \vec{E} is much stronger than the one on \vec{B} , which will make it very hard to discover the latter at the LHC [2].

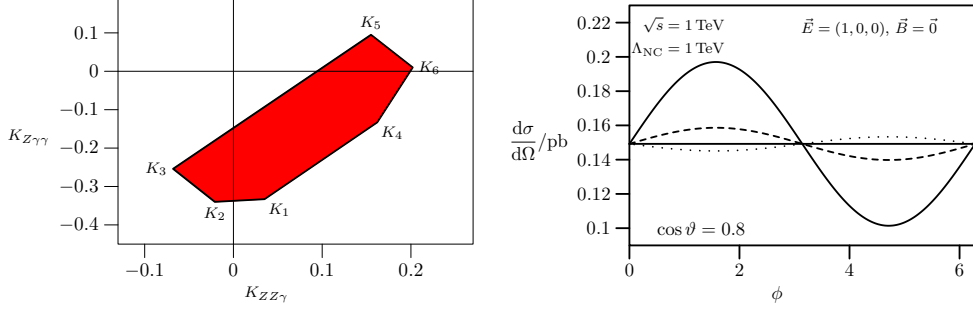


Figure 1: Left: The allowed region for the values of the couplings $K_{Z\gamma\gamma}$ and $K_{ZZ\gamma}$ in the nonminimal NCSM. Right: Azimuthal dependence of the cross section for $e^+e^- \rightarrow Z\gamma$, in the nonminimal NCSM with different values for the TGB couplings: $K_1 = (-0.333, 0.035)$ (solid) and $K_5 = (0.095, 0.155)$ (dotted), and in the minimal NCSM (dashed).

2.2 Dependence on the Coupling Constants

Since the t - and u -channel diagrams as well as the contact term are proportional to Q^2 , Q being the particle charge in the initial state, the cross section in the minimal NCSM depends only on the modulus $|Q|$. In contrast, in the nonminimal NCSM, the interference with the s -channel diagrams adds a Q^3 term to the cross section and the cross section also depends on $\text{sgn}(Q)$. As a result, NC effects in $e^+e^- \rightarrow Z\gamma$ are maximally enhanced by the s -channel contribution for the pairs of couplings K_1 and K_2 , corresponding to the lower edge of the polygon in Figure 1, left. However, the same couplings lead to cancellations of the NC effects for $u\bar{u}$ scattering resulting in minimal deviations of the NCSM with respect to the SM. In this sense, the ILC will nicely complement the LHC. On the other hand, the pair of couplings K_5 , which produces maximal effects at the LHC, will lead to an NCSM cross section comparable to the one where the TGB couplings vanish.

2.3 Monte Carlo Simulations for the ILC

In order to estimate the sensitivity of the ILC on the NC scale Λ_{NC} , we have performed Monte Carlo simulations using the event generator WHIZARD [6]. In the analysis we used a center of mass energy of $\sqrt{s} = 500$ GeV and an integrated luminosity of $\mathcal{L} = 500 \text{ fb}^{-1}$.

A typical signature for new physics is a modified p_T -distribution. Previously, we have studied $pp \rightarrow Z\gamma \rightarrow e^+e^-\gamma$ at the LHC and the deviation from the SM $p_T(\gamma)$ distribution could not be resolved due to the poor statistics and complicated cuts [2]. However, the high statistics and the clean initial state of the ILC, allows deviations of the NCSM from the SM to be seen also in the p_T distribution for reasonable values of Λ_{NC} (see Figure 2, left). Of course, cuts with respect to the azimuthal angle ϕ have to be applied, because otherwise all $\mathcal{O}(\theta)$ interference effects will cancel, since the events “missing” in one hemisphere (e.g. for $\pi < \phi < 2\pi$) are compensated by the “excess” of events in the other. Figure 2, right, shows this distribution exemplarily, where for the TGB couplings we have chosen the set of values, for which we expect the largest deviation from the SM distribution in electron-positron scattering, i.e. K_1 .

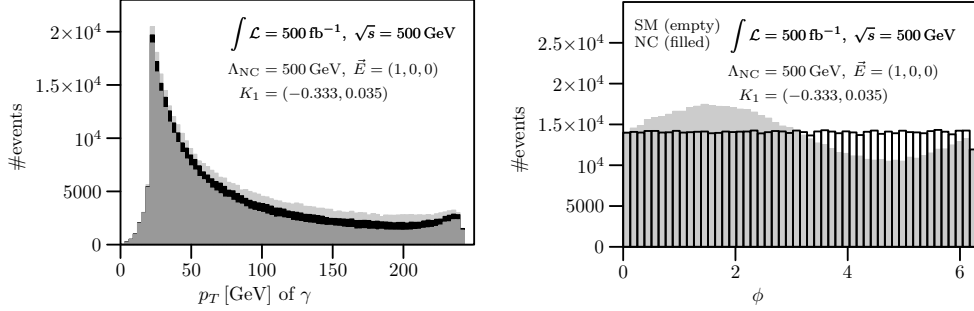


Figure 2: Left: Monte Carlo simulation for the photon p_T distribution in the process $e^+e^- \rightarrow Z\gamma$ at the ILC showing the distribution in the NCSM for $0.0 < \phi < \pi$ ($\pi < \phi < 2\pi$) above (below) the black SM histogram. Right: Monte Carlo simulation for the azimuthal dependence of the process $e^+e^- \rightarrow Z\gamma$ at the ILC.

As shown in [2], the strong boost along the beam axis from the partonic to the hadronic CMS at the LHC induces kinematical correlations between (E_1, B_2) and (E_2, B_1) , respectively. Thus, in the laboratory frame we always deal with an entanglement of time- and space-like noncommutativity. Fortunately, the different properties of the \vec{E} and \vec{B} parameters with respect to the partonic scattering angle discussed in section 2.1 allows separate measurements of the time- and space-like components of θ . Integrating just over one hemisphere (i. e. $-0.9 < \cos \vartheta^* < 0$ or $0 < \cos \vartheta^* < 0.9$) we can perform a measurement of \vec{E} , since the \vec{B} dependence is negligibly small. On the other hand, an integration over the whole sphere (i. e. $-0.9 < \cos \vartheta^* < 0.9$) in principle provides a pure measurement of \vec{B} , since the effect of \vec{E} will completely cancel out, due to its antisymmetry.

One advantage of the ILC compared to the LHC is the only mildly boosted initial state. We have an e^+e^- initial state, where only beamstrahlung has to be accounted for, which we have done, using CIRCE [7] inside WHIZARD [6]. This will lead to a boost of the CMS of the electrons to the laboratory frame. Yet, compared to the LHC, this boost is negligibly small: $\langle |\beta_{\text{ILC}}| \rangle = 0.14$ versus $\langle |\beta_{\text{LHC}}| \rangle = 0.8$. We therefore have negligible correlations between E_1 and B_2 or E_2 and B_1 , respectively, and we can derive the bounds on Λ_{NC} separately for the case of purely \vec{E} or purely \vec{B} noncommutativity.

3 Results and Conclusions

Focussing on the azimuthal dependency (Figure 2) we have performed likelihood fits similar to the ones described in [2] in order to derive bounds on the NC scale Λ_{NC} . The results are summarized in Table 1. In contrast to the LHC case, the ILC is sensitive on all noncommutative parameters, time-like and space-like, as well as on all values of the TGB couplings. The ILC is especially sensitive on the couplings lying in the lower region of the polygon of Figure 1. These are exactly the set of TGB couplings for which the LHC is less sensitive, while the TGB couplings leading to maximal deviations at the LHC, lead to minimal effects at the ILC. Thus, probing the TGB couplings at the ILC is complementary to searches at the LHC. If a noncommutative structure of space-time exists in nature at a scale of the order

$(K_{Z\gamma\gamma}, K_{ZZ\gamma})$	$ \vec{E} ^2 = 1, \vec{B} = 0$	$\vec{E} = 0, \vec{B} ^2 = 1$
$K_0 \equiv (0, 0)$	$\Lambda_{\text{NC}} \gtrsim 2 \text{ TeV}$	$\Lambda_{\text{NC}} \gtrsim 0.4 \text{ TeV}$
$K_1 \equiv (-0.333, 0.035)$	$\Lambda_{\text{NC}} \gtrsim 5.9 \text{ TeV}$	$\Lambda_{\text{NC}} \gtrsim 0.9 \text{ TeV}$
$K_5 \equiv (0.095, 0.155)$	$\Lambda_{\text{NC}} \gtrsim 2.6 \text{ TeV}$	$\Lambda_{\text{NC}} \gtrsim 0.25 \text{ TeV}$
$K_3 \equiv (-0.254, -0.048)$	$\Lambda_{\text{NC}} \gtrsim 5.4 \text{ TeV}$	$\Lambda_{\text{NC}} \gtrsim 0.9 \text{ TeV}$

Table 1: Bounds on Λ_{NC} from $pp \rightarrow Z\gamma \rightarrow e^+e^-\gamma$ at the LHC, for the minimal (first row) and nonminimal NCSM

of 1 TeV without being discovered at the LHC because of an unfavorable value of the TGB coupling (i. e. in the upper part of the polygon in Figure 1), then the ILC will see it.

4 Acknowledgments

This research is supported by Deutsche Forschungsgemeinschaft (grant RU 311/1-1 and Research Training Group 1147 *Theoretical Astrophysics and Particle Physics*) and by Bundesministerium für Bildung und Forschung BMBF (grant 05H4WWA/2). A. A. gratefully acknowledges support from Evangelisches Studienwerk e. V. Villigst. A. A. thanks the members of SLAC Theory Group for their kind hospitality.

References

- [1] Slides:
<http://ilcagenda.linearcollider.org/contributionDisplay.py?contribId=237&sessionId=72&confId=1296>
- [2] A. Alboteanu, T. Ohl and R. Rückl, Phys. Rev. **D74**, 096004 (2006) [arXiv:hep-ph/0608155]; PoS **HEP2005** (2006), 322 [arXiv:hep-ph/0511188].
- [3] X. Calmet, B. Jurčo, P. Schupp, J. Wess and M. Wohlgenannt, Eur. Phys. J. **C23**, 363 (2002) [arXiv:hep-ph/0111115]; B. Melic, K. Passek-Kumericki, J. Trampetic, P. Schupp and M. Wohlgenannt, Eur. Phys. J. **C 42**, 483 (2005) [arXiv:hep-ph/0502249]; B. Melic, K. Passek-Kumericki, J. Trampetic, P. Schupp and M. Wohlgenannt, Eur. Phys. J. **C 42**, 499 (2005) [arXiv:hep-ph/0503064].
- [4] A. Alboteanu, T. Ohl and R. Rückl, arXiv:0707.3595 [hep-ph].
- [5] T. Ohl and J. Reuter, Phys. Rev. **D70**, 076007 (2004) [arXiv:hep-ph/0406098]; T. Ohl and J. Reuter [arXiv:hep-ph/0407337].
- [6] W. Kilian, T. Ohl and J. Reuter, arXiv:0708.4233 [hep-ph]; M. Moretti, T. Ohl and J. Reuter, [arXiv:hep-ph/0102195]; W. Kilian, LC-TOOL-2001-039.
- [7] T. Ohl, Comput. Phys. Commun. **101**, 269 (1997) [arXiv:hep-ph/9607454].